HIPPOCAMPUS 27:115–121 (2017)

RAPID COMMUNICATION

Dissociable Profiles of Generalization/Discrimination in the Human Hippocampus During Associative Retrieval

Natalie G. De Shetler[1] and Jesse Rissman[1,2,3,4]*

ABSTRACT: When encountering stimuli that vary slightly from previous experiences, neural signals within the CA_3 and dentate gyrus (CA_3DG) hippocampal subfields are thought to facilitate mnemonic discrimination, whereas CA_1 may be less sensitive to minor stimulus changes, allowing for generalization across similar events. Studies have also posited a critical role for CA_1 in the comparison of events to memory-derived expectations, but the degree to which these processes are impacted by explicit retrieval demands is yet unclear. To evaluate extant accounts of hippocampal subfield function, we acquired high-resolution fMRI data as participants performed a task in which famous names were used to cue the retrieval of previously paired images. Although both left CA_3DG and CA_1 showed match enhancement effects, responding more to original paired images (targets) than to never-before-seen images (novels), the sensitivity of these subfields to stimulus changes and task demands diverged. CA_3DG showed a goal-independent, yet highly specific, preference for previously encountered stimuli, responding equally strongly to targets and mispaired associates, while showing equally weak responses to close lures and novels. In contrast, recognition signals in CA_1 were goal-dependent (i.e., not evoked by mispaired associates), yet accommodating of subtle stimulus differences, such that close lures evoked comparable activity as targets. © 2016 Wiley Periodicals, Inc.

KEY WORDS: hippocampal subfields; associative memory; mismatch detection; high-resolution fMRI; pattern separation/pattern completion

INTRODUCTION

One fruitful approach for characterizing mnemonic processing within distinct hippocampal subfields has been to measure neural responses to stimuli that closely, but not exactly, match a previously encountered item or association. If a region's response to these "close lure" stimuli mimics its response to novel stimuli, the region is said to show a discrimination effect. This is sometimes referred to as pattern separation (Yassa and Stark, 2011; Deuker et al., 2014), since the close lure must be encoded in such a manner as to minimize its representational overlap with the previously learned stimulus, thus preventing catastrophic mnemonic interference (Kesner, 2013a,c). Previous high-resolution functional MRI (hr-fMRI) studies have predominantly observed mnemonic discrimination effects in the CA_3 and dentate gyrus subfields of the hippocampus (Bakker et al., 2008; Lacy et al., 2011). Because most hr-fMRI protocols lack the resolution to differentiate between these regions (Carr et al., 2010), we will follow the convention of referring to them as a combined CA_3DG region.

Mnemonic generalization effects, on the other hand, have been reported in the downstream hippocampal subfield of CA_1, which responds similarly to close lure stimuli and exact repeats of a past stimulus (Bakker et al., 2008; Lacy et al., 2011). Such generalization possibly reflects pattern completion mechanisms that facilitate recall based on degraded stimuli (Kesner, 2013b,c). CA_1 activity levels have been shown to scale linearly with the degree to which a present stimulus deviates from a past version (Leutgeb et al., 2005; Lacy et al., 2011), but this region may be minimally sensitive or insensitive to very subtle perceptual differences. Extant fMRI-based demonstrations of this dissociation between CA_3DG and CA_1 rely on incidental recognition paradigms (i.e., tasks requiring no actual memory judgments) making it challenging to evaluate the degree to which mnemonic encoding and/or retrieval operations drive these respective response profiles (Deuker et al., 2014; Liang and Preston, 2015).

Several fMRI studies have examined hippocampal sensitivity to whether events match or mismatch one's memory-based expectation (e.g., associative novelty) (Kumaran and Maguire, 2006, 2007a; for reviews: Kumaran and Maguire, 2007b, 2009), and those using hr-fMRI have typically reported effects in the CA_1 region (Chen et al., 2011, 2015; Duncan et al., 2012). Since CA_1 receives direct inputs from CA_3, putatively conveying associative information derived from CA_3-mediated pattern completion, and from entorhinal cortex, putatively conveying information about sensory reality (Amaral and Witter, 1989; Amaral, 1993), CA_1

[1] Department of Psychology, University of California Los Angeles, Los Angeles, California; [2] Department of Psychiatry and Biobehavioral Sciences, University of California Los Angeles, Los Angeles, California; [3] Brain Research Institute, University of California Los Angeles, Los Angeles, California; [4] Integrative Center for Learning and Memory, University of California Los Angeles, Los Angeles, California
*Correspondence to: Jesse Rissman, 1285 Franz Hall, Box 951563, Los Angeles, CA 90095-1563, USA. E-mail: rissman@psych.ucla.edu
Accepted for publication 16 November 2016.
DOI 10.1002/hipo.22684
Published online 18 November 2016 in Wiley Online Library (wileyonlinelibrary.com).

is uniquely situated to compare these two signals and evaluate whether one's memory-based expectation is consistent with the current state of the world (Vinogradova, 2001). Furthermore, CA_1 connects to a larger reward/motivation system that allows for memory modulation in response to both external cues (such as mnemonic mismatches) and internal drives (Lisman and Grace, 2005). Indeed, when subjects are explicitly tasked with judging whether a probe stimulus matches a past memory, match enhancement (repeat > novel) signals are typically observed throughout the hippocampus (Hannula and Ranganath, 2008; Duncan et al., 2009) and are especially pronounced in CA_1 (Dudukovic et al., 2011; Duncan et al., 2012). Some studies using explicit tasks, however, find mismatch enhancement effects (Chen et al., 2011; Duncan et al., 2012).

We conducted an hr-fMRI study to determine if the previously described profile of mnemonic discrimination in CA_3DG and generalization in CA_1 persists in an explicit associative memory recall task and, furthermore, how the demands of the task affect these patterns. Subjects were scanned while performing a delayed paired associate memory test assessing their recollection of arbitrarily paired celebrity names and image associates learned the previous day (Fig. 1A). Each test trial presented a celebrity name, and participants first rated the strength of their memory for the visual associate and then several seconds later judged whether a probe image was either (1) the original paired image (*target*), (2) a different exemplar of the original image (*lure)*, or (3) a very different image from what had been studied with that name. Images from this final condition were either never before seen (*novel*) or had been paired with a different name (*mispaired*). Hand-drawn regions of interests (ROIs) allowed for the characterization of hippocampal subfield activity during the presentation of these probes, following previous ROI creation and data extraction protocols (Chen et al., 2011). See Detailed Methods for more information about the task paradigm and MRI data acquisition and analysis procedures.

Subjects correctly determined probe type on 58.3% (SD = 16.5%) of trials, which far exceeded chance-level (25%) responding ($t_{(25)} = 10.61$, $P < 0.001$). Although accuracy differed between conditions ($F_{(3,72)} = 3.748$, $P = 0.015$), only identification of novel images (mean = 70.00%, SD = 19.17%) was greater than the other conditions (target: mean = 58.33%, SD = 21.37%, $t_{(24)} = 2.62$, $P = 0.015$; lure: mean = 57.92%, SD = 18.34%; $t_{(24)} = 2.68$, $P = 0.013$; mispaired: mean- = 59.33%, SD = 20.42%, $t_{(24)} = 3.28$, $P = 0.003$); there was no difference between the remaining conditions ($F_{(2,48)} = 0.057$, $P = 0.945$) (Fig. 1B). Furthermore, on correct trials, response times (RTs) varied by probe type ($F_{(3,72)} = 25.659$, MSE = 0.009, $P < 0.001$), reflecting faster RTs for detecting target probes (mean = 1.24 sec, SD = 0.17) or novels (mean = 1.29 sec, SD = 0.19) than either lures (mean = 1.40 sec, SD = 0.16; vs. targets: $t_{(24)} = 6.87$, $P < 0.001$; vs. novels: $t_{(24)} = 4.81$, $P < 0.001$) or mispaired probes (mean = 1.45 sec, SD = 0.24; vs. targets: $t_{(24)} = 6.59$, $P < 0.001$; vs. novels: $t_{(24)} = 5.97$, $P < 0.001$). Subjective memory strength ratings, reported in response to the cue stimulus, were strongly related to the accuracy of participants' probe responses ($F_{(3,18)} = 24.83$, $P < 0.001$). However, there was no apparent confound between subjective memory strength ratings and probe type, as mean strength ratings (when coded on a numerical scale: 4 = strong memory, 1 = no memory) did not differ between the four probe types (target mean = 2.60, SD = 0.60; lure: mean = 2.60, SD = 0.60; mispaired: mean = 2.62, SD = 0.55; novel: mean = 2.57, SD = 0.69; $F_{(3,72)} = 0.45$, $P = 0.719$), and there was no interaction between memory rating and probe type on accuracy ($F_{(9,54)} = 0.03$, $P = 0.611$).

To confirm previous findings that the hippocampus shows differential responses to novel items relative to, in this case, correctly paired targets, we contrasted the fMRI activation parameter estimate maps associated with these two probe conditions (all analyses are restricted to trials where participants indicated the correct response). Consistent with findings of stronger activation for items that match expectations in a task (Dudukovic et al., 2011; Duncan et al., 2012), we found a significant cluster within the left hippocampus (58 continuous voxels, Z-max = 3.44 at [−24 −22 −18], $P = 0.007$, small volume corrected) that showed greater activity for target probes than for novel probes (Fig. 2A). No hippocampal clusters emerged for novels > targets, indicating that hippocampal novelty detection and/or repetition suppression effects observed in prior studies using incidental recognition tasks (e.g., Bakker et al., 2008; Lacy et al., 2011) may not be characteristic of explicit retrieval tasks like ours. Furthermore, these analyses revealed no significant findings in the right hippocampus. Thus, we elected to focus our subfield ROI analyses exclusively on the left hippocampus, which may have shown more robust effects in our task due to subjects' reliance on verbal/semantic processing to promote the memorability of name-image associations.

Following methods employed by Chen et al. (2011), in order to increase the sensitivity of our ROI analyses, we first identified a subset of task-responsive voxels within each region, based on a statistically independent analysis of the incorrect trials (which were not included in our analyses of interest). For each subject, we identified the top 25% of voxels across each ROI that showed the greatest response to probes on incorrect trials (collapsed across probe conditions) compared to baseline; in so doing, we ensured that our ROIs were comprised of voxels that were at least modestly engaged during the probe period. Probe activity estimates for correct trials were then extracted from the resulting ROIs for all probe conditions (Fig. 3). Both the left CA_1 ($F_{(1,24)} = 6.406$, $P = 0.018$) and CA_3DG ($F_{(1,24)} = 9.964$, $P = 0.004$) showed significantly greater activity to targets than novel probes. Although our core hypotheses were concerned with the activation profile of the CA fields, we also examined effects within the left subiculum, the primary output structure of the hippocampus. This region showed no difference in activity between target and novel probes ($F_{(1,24)} = 0.331$, $P = 0.570$).

Within the context of match enhancement, we next examined the degree to which these two subfields exhibit activity patterns reflecting generalization or discrimination, and the task sensitivity of these patterns. The relative activity of the

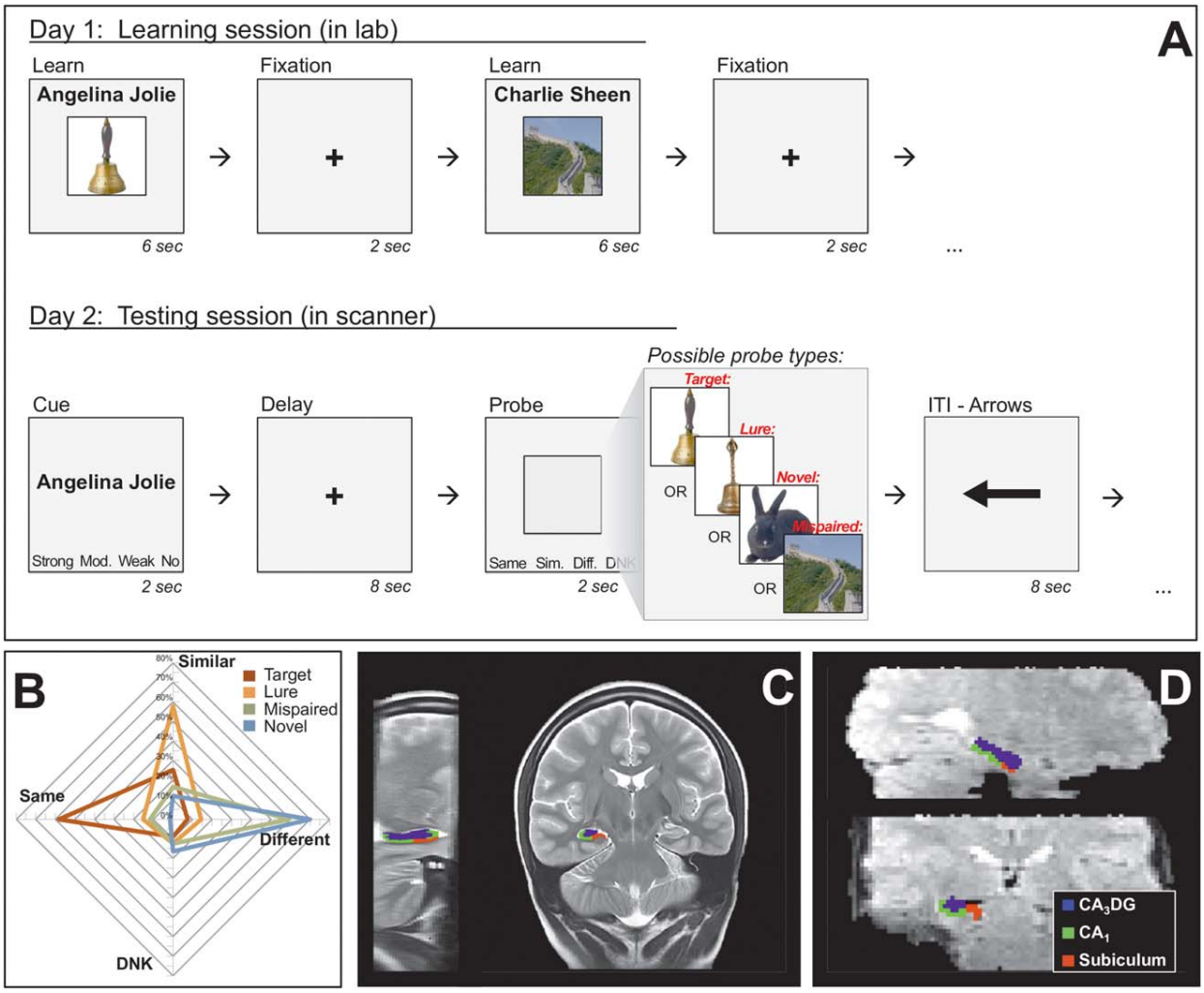

FIGURE 1. (A) Experimental design. During the learning phase, subjects viewed 168 randomly generated name/image pairs and were instructed to memorize the association between each pair. All pairs were presented twice. The testing phase was conducted the next day while fMRI data were collected. Each trial began with the presentation of a celebrity name cue, and participants rated the strength of their memory for the image associate. Then, following an 8 sec delay, a probe image was presented and subjects were to respond whether the probe was the exact same picture that they had previously associated with the name, or whether it was a similar picture, a very different picture, or that they "do not know" (DNK). Examples of the four probe conditions (target, lure, novel, or mispaired) are provided for illustration. (B) Distribution of behavioral responses by condition types. (C) Example hand-drawn hippocampal subfield ROIs (only left hemisphere shown) overlaid on the template high-resolution coronal structural image. (D) Example ROIs (only left hemisphere shown) following transformation to native EPI space, overlaid on a single EPI volume. [Color figure can be viewed at wileyonlinelibrary.com]

lure probes compared to target and novel probes allows us to determine if a region generalizes (i.e., shows comparable activity for lure and target images) or discriminates (i.e., shows comparable activity for lure and novel images). The mispaired, but pre-exposed, probe images can provide insight into the expectation dependency of a region's match enhancement effect. For instance, a region's mnemonic recognition signals could be expectation-dependent, showing increased activity only for correctly paired images, or expectation-independent, where any previously seen image elicits match enhancement (i.e., comparable activity for mispaired and target images). Figure 2B summarizes four hypothetical profiles of expectation dependency and discrimination.

To evaluate whether left CA_3DG and CA_1 showed dissociable profiles of responding, we first tested for a region $\times$ probe condition interaction, which showed a marginally significant effect ($F_{(3,72)} = 2.643$, $P = 0.056$). Given that our previous analyses showed greater activity for target probes relative to novels in both subfields, we next sought to evaluate whether the two subfields would show dissociable effects when only considering their responses across the other three probe conditions, which each involve some degree of mnemonic mismatch

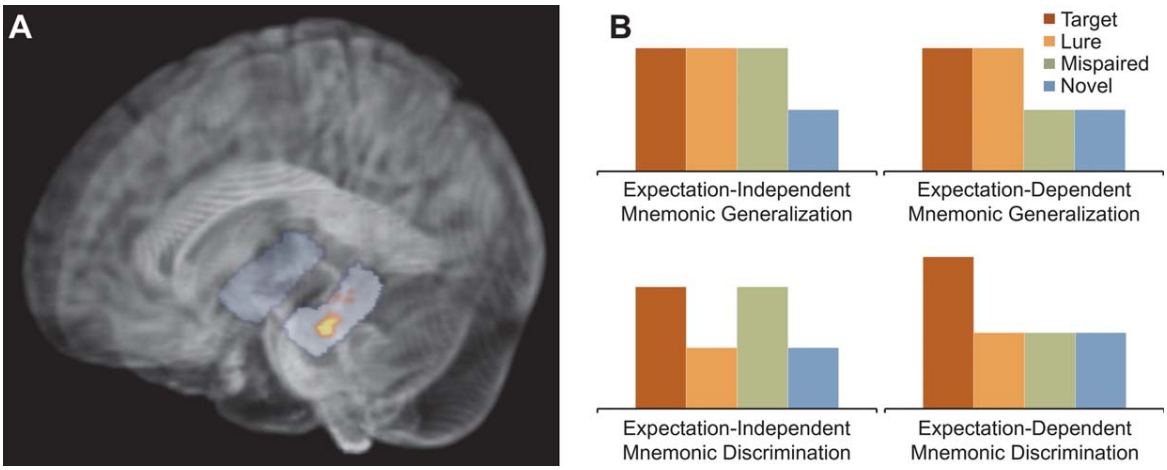

FIGURE 2. (A) Group-level contrast of target and novel probe stimuli within a whole hippocampus mask. Only one cluster in left hippocampus achieved significance for targets > novels. No clusters showed the reverse effect. (B) Four hypothetical response patterns for combinations of expectation dependency and mnemonic discrimination. Expectation-dependent regions should respond less to previously seen but mispaired images, essentially treating these images as novel images. Expectation-independent regions would respond to mispaired images as they would to any other previously seen image, thus showing similar responses as to targets. Discriminating regions are expected to reject lure images, responding at similar levels as novels, while generalizing regions will show comparably high activity to lures and targets. [Color figure can be viewed at wileyonlinelibrary.com]

to the previously learned associate. This interaction proved significant ($F_{(2,48)} = 3.452$, $P = 0.040$), indicating that CA_3DG and CA_1 show a differential responsivity to lure, mispaired, and novel images.

In both regions, we next compared responses to lure probes to those elicited by target or novel probes. In CA_1 lures did not differ from targets ($F_{(1,24)} = 0.139$, $P = 0.713$), while they did differ from novels ($F_{(1,24)} = 5.734$, $P = 0.025$). In contrast, in CA_3DG lures differed significantly from targets ($F_{(1,24)} = 6.063$, $P = 0.021$), but showed no difference from novels ($F_{(1,24)} = 0.440$, $P = 0.513$), Figure 3. This finding comports with results from prior studies that found sensitivity to subtle visual changes in CA_3DG and sensitivity to larger changes in CA_1 (Bakker et al., 2008; Lacy et al., 2011).

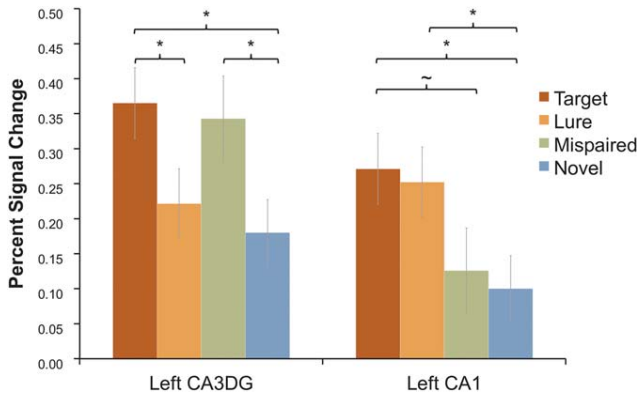

FIGURE 3. Mean percent signal change within left CA1 and CA3DG ROIs as a function of probe type. Both regions show greater response to targets than novels. Similarly, previously seen but mispaired images evoked greater response within the CA3DG than novel images, but did not differ from targets. CA1 responses did not differ between mispaired and novel images, but mispaired images showed a trend towards reduced activation compared to targets. Furthermore, CA1 responses to lures were greater than to novels and did not differ from targets; in the CA3DG, activation to lures did not differ from novels, but was less than activation to targets. All error bars show standard error of the mean. [Color figure can be viewed at wileyonlinelibrary.com]

We next contrasted mispaired probes with target and novel probes. CA_3DG showed increased activity for mispaired images compared to novel ($F_{(1,24)} = 11.935$, $P = 0.002$), but did not differ from targets ($F_{(1,24)} = 0.134$, $P = 0.718$), reflecting a generalized preference for familiar stimuli, regardless of whether the specific probe image was expected (i.e., targets) or unexpected (i.e., mispaired) in the context of a given trial. CA_1, however, showed no difference between mispaired and novel probes ($F_{(1,24)} = 0.127$, $P = 0.725$), but showed a trend towards mispaired probes evoking less activity than targets ($F_{(1,24)} = 3.829$, $P = 0.062$). Thus, CA_1 showed high activity on trials where the probe stimulus was either an exact match (targets) or near match (lures) to one's memory-based expectation, but lower activity on trials where the probe's content was unanticipated. Importantly, this effect was observed regardless of whether the unexpected probe stimulus was truly novel or whether it was merely contextually novel (previously seen in the context of a different name-image pairing).

The findings here conform with prior fMRI work showing that the CA_3DG subfield of human hippocampus responds to lure images as it would to novel images (discrimination), whereas CA_1 responds to lures as it would to repeated images (generalization) (Bakker et al., 2008; Lacy et al., 2011). However, unlike previous studies which observed these dissociable subfield response profiles in the broader context of repetition

suppression effects (decreased activity to targets), here we document a similar dissociation in the context of match enhancement effects (increased activity to targets). Furthermore, the activity increase to targets we observe in both subfields aligns with earlier work showing increased activity to matching conditions when subjects were explicitly tasked with evaluating the whether the probe stimulus matched or mismatched one's expectations (Hannula and Ranganath, 2008; Duncan et al., 2009, 2012; Dudukovic et al., 2011).

Importantly, our results demonstrate dissociable hippocampal response profiles as a function of condition. CA_3DG discriminates old visual stimuli from new stimuli, irrespective of the task-relevant expectations. That is, it shows the same degree of match enhancement to all previously encountered images, regardless of their associative relationship to the name recall cue. In contrast, CA_1 responds to incorrectly paired targets as it would to completely novel probes, while it generalizes to different exemplars of the expected image. This may reflect top-down, goal-directed, influences on CA_1 responses. Given the structure of our task, subjects likely retrieve and maintain a generic semantic description of the target (e.g., "gold bell") in addition to any specific visual details that may come back to mind. The CA_1 region appears to play a role in detecting when the probe stimulus matches one's general memory-based prediction. However, in studies using incidental tasks where subjects are not given a goal of making memory judgments, CA_1 may favor novelty because stimuli that violate one's expectations may be more motivationally salient in such a context. As our paradigm lacks an experimental manipulation of task demands (i.e., we did not have a condition where probe recognition was incidental), we cannot definitively conclude that our data demonstrate a task-specific effect.

Our results further emphasize the challenges inherent in attributing the differential lure sensitivity of the CA_3DG and CA_1 subfields to pattern separation and pattern completion mechanisms, given that these mechanisms are typically associated with encoding and recall processes, respectively (Hunsaker and Kesner, 2013). In order to correctly report that a lure probe was similar, but not identical, to the studied image, subjects likely adopted a "recall-to-reject" strategy (Rotello and Heit, 2000). Within the context of this strategy, increased activity within the CA_1 to close lures could actually reflect pattern completion processes. However, the fact that CA_3DG showed comparably high responses to targets and mispaired probes does not necessarily fit with a pattern separation account, which might have predicted high responses to novels and lures (indicative of encoding processes) and lower responses to already-familiar stimuli (targets and mispaired images). Rather, it seems more plausible that CA_3DG responses in our task reflect highly specific signaling that a probe stimulus is an exact match to a past experience, regardless of whether that stimulus was expected based on the cued name associate.

Without more conditions presenting additional degrees of perceptual dissimilarity for lure images, we cannot say with certainty that the increased activity to both targets and lures observed in CA_1 reflects insensitivity to lures. As previous research shows that CA_1 linearly tracks the amount of change in stimuli and environments (Leutgeb et al., 2005; Lacy et al., 2011), we possibly would have observed a more graded effect had we added another level of lure dissimilarity. Furthermore, previous research (Chen et al., 2011; Dudukovic et al., 2011) has demonstrated that responses within the MTL may depend in part on the stimulus category of the mismatching probes (e.g., faces vs. scenes), but low trial counts when subdividing our probes based on stimulus category preclude our examinations of such effects. Future investigations should evaluate the degree to which the effects reported here might be modulated by probe category. Finally, our experiment lacked power to allow examination of the potentially informative responses of the hippocampal subfields to lure trials that subjects either misidentified as "same" (over-generalization) or "different" (over-discrimination), nor did we have sufficient trials to examine the effect of subjectively reported memory strength on our pattern of results. Future efforts more focused on these questions could illuminate hippocampal subfield contributions to subjective experiences leading to over-generalization and/or forgetting, as well as the modulation of mismatch responses by prediction strength (Chen et al., 2015).

DETAILED METHODS

Participants

Twenty-nine right-handed healthy members of the University of California, Los Angeles (UCLA) community participated in this study. Participants consented and received compensation in compliance with the UCLA Institutional Review Board. Four subjects' data were excluded due to issues affecting data quality. In total, 25 participants make up this data set (13 females; mean age = 20.6; range: 18–24 years).

Task Design

Our task was comprised of two parts: a learning phase and a testing phase (Fig. 1A). During the learning phase, subjects were presented with 168 randomly generated name/image associations, each consisting of a celebrity's name and a visual image of an object, an animal, or a building/landmark. Each pair was displayed for 6 sec, and subjects were told to explicitly form an associative memory connecting the name with the image. The session included two study rounds, such that each pair was encountered twice. On the following day, participants returned for an fMRI scanning session, during which their memory for the associations was tested. Each trial began with the presentation of a celebrity name, and subjects were to mentally recall the associated image and rate the strength of their memory on a 4-level scale: "Strong" to "No" memory. After an 8 sec delay, a probe image was presented for 2 sec. Probe stimuli could either be the previously learned image associate (*targets*), a similar image to the learned associate (i.e., a

different exemplar of the same item; *lures*), or a very different image than the learned associate (i.e., an exemplar from a different visual category). For this final class of probes, half had been previously encountered during the learning phase, but associated with a different celebrity name, withheld from the testing (*mispaired*) and half were presented for the first time during the test phase (*novels*). Subjects were to make a button-press response indicating whether they thought the probe was an: "Exact match" (the correct response for targets), "Similar" (correct for lures), "Very Different" (correct for novels *and* mispaired probes), or "Do Not Know" (a response option included to discourage guessing). Subjects performed a total of 144 memory trials (48 targets, 48 lures, 24 mispaired, and 24 novels; each of the 168 name cues appeared once, with the exception of 24 names that were withheld because their image associates were used as mispaired probes). In an effort to prevent mind-wandering during the inter-trial interval, which can be associated with hippocampal activity (Stark and Squire, 2001), subjects performed an active baseline task for 8 sec between trials, requiring them to report the right/left direction of a series of arrow stimuli.

MRI Data Acquisition

Neuroimaging data were acquired on a 3.0T Siemens Tim Trio MRI system equipped with a 12-channel receive-only phased array head coil at the UCLA Staglin IMHRO Center for Cognitive Neuroscience. Functional scans used a T2*-weighted gradient-echo planar imaging (EPI) pulse sequence (repetition time (TR) = 2,500 ms; echo time (TE) = 28 ms; GRAPPA acceleration factor = 2; 38 slices aligned off angle to the hippocampal long axis; 1.7 × 1.7 × 1.8 mm voxel size; eight runs; 146 volumes per run). A T1-weighted magnetization-prepared rapid-acquisition gradient echo (MPRAGE; 240 sagittal slices, 1 × 1 × 1 mm voxels) acquired anatomical images of the whole brain. A T2*-weighted high-resolution anatomical scan of the hippocampus (28 slices aligned perpendicular to the long axis of the hippocampus, 0.4 × 0.4 × 1.8 mm voxels) allowed for subfield ROI creation. MRI-compatible LCD goggles presented visual stimuli, and a four-button box recorded subjects' responses.

Region of Interest Creation and Data Preprocessing

Hippocampal ROIs for the right and left CA_1, $CA_{2/3/}$ dentate gyrus (which, following convention, we abbreviate as CA_3DG), and subiculum were hand traced for each subject on their high-resolutional coronal structural image across the entire length of the hippocampus following conventional region boundaries (Duvernoy et al., 2013; Frankó et al., 2014), Figure 1C. Working from anterior to posterior, hippocampal tissue prior to the appearance of digitations was designated as CA_1 (typically the 1–2 anteriormost slices). For the remainder of the hippocampal head, CA_1 was delineated from the subiculum by drawing a line down from the most ventral point of the stratum radiatum/lacunosum-moleculare, and the CA_1/CA_3DG division was drawn where the CA band began to thin, representative of the transition from CA_1 to CA_2. Throughout the hippocampal body, the CA_1/CA_3DG division continued to be defined by the thinning of the CA band, while the CA_1/subiculum border was defined by a line perpendicular to the outer boundary of the subiculum to the medial border of the hippocampus. ROIs for MTL cortices were created, but were not employed in this study due to inconsistent coverage and signal drop out resulting from the angle of functional acquisition. All fMRI BOLD data extraction analyses were performed in native EPI space, and several registration steps using Advanced Normalization Tools (ANTs) (Avants et al., 2010, 2011) transformed the ROIs into this space, Figure 1D. Template EPI space created for each subject based on exemplar images from each of the eight scanner runs accommodated any small drifts resulting from subject motion over the course of the scanning session, and transforms of each EPI run to the template were calculated. Both the template and the high-res hippocampal image were aligned to subject's MPRAGE image. ROIs created in the high-res anatomical space were moved directly to EPI space by applying the appropriate set of transformation parameters. An additional transform of subject MPRAGE to a study specific whole-brain template moved EPI images to a common space for the creation of group maps.

The data were slice time corrected, and motion and magnetic field distortion corrections were performed concurrently using FSL's (Jenkinson et al., 2012) FLIRT (Jenkinson et al., 2002) (FMRIB's Linear Image Registration Tool) and field unwarping tool (FUGUE). To prevent the blending of activity across neighboring hippocampal subfields, the data used in the ROI analyses were not spatially smoothed. However, when generating group-level activity maps, a 5 mm Gaussian FWHM smoothing kernel was applied the EPI data to accommodate across-subject variability in subfield boundaries.

fMRI Data Analysis

All statistical modeling was performed with FSL's FEAT (FMRI Expert Analysis Tool). Our general linear model (GLM) investigating activity during probe presentation consisted of six regressors, represented by 2-sec boxcars convolved with a gamma hemodynamic response function, one each for successfully classified probes based on probe type (target, lure, mispaired, novel), one for all incorrect trials collapsed across trial types, and one for the cue period. The ITI period remained unmodeled and served as an "active baseline" (Stark and Squire, 2001). Six head motion parameters, as well as their first and second derivatives, were included as regressors of no interest. This resulted in activity parameter estimates (betas) for each subject for all task conditions occurring during each run.

For subfield ROI analyses, betas were converted to percent signal change (Mumford, 2007), representing each condition's change from baseline. Signal change estimates within each ROI were extracted for conditions in each run, and a weighted average based on the number of trials per run was then calculated to generate across-run mean signal change estimates. For the voxelwise

mapping analysis, first-level GLMs were performed on smoothed data, then fixed effects were calculated to combine parameter estimates across runs, and finally, mixed effects group contrasts were calculated across subjects using FSL's FLAME1 method. Clusters were thresholded at $P < 0.05$ FWE-corrected, accounting for the empirical smoothness of the group residuals, using a whole hippocampus mask for small volume correction.

REFERENCES

Amaral DG. 1993. Emerging principles of intrinsic hippocampal organization. Curr Opin Neurobiol 3:225–229.

Amaral DG, Witter MP. 1989. The three-dimensional organization of the hippocampal formation: A review of anatomical data. Neuroscience 31:571–591.

Avants BB, Tustison NJ, Song G, Cook PA, Klein A, Gee JC. 2011. A reproducible evaluation of ANTs similarity metric performance in brain image registration. NeuroImage 54:2033–2044.

Avants BB, Yushkevich P, Pluta J, Minkoff D, Korczykowski M, Detre J, Gee JC. 2010. The optimal template effect in hippocampus studies of diseased populations. NeuroImage 49:2457–2466.

Bakker A, Kirwan CB, Miller M, Stark CEL. 2008. Pattern separation in the human hippocampal CA3 and dentate gyrus. Science 319: 1640–1642.

Carr VA, Rissman J, Wagner AD. 2010. Imaging the human medial temporal lobe with high-resolution fMRI. Neuron 65:298–308.

Chen J, Cook PA, Wagner AD. 2015. Prediction strength modulates responses in human area CA1 to sequence violations. J Neurophysiol 114:1227–1238.

Chen J, Olsen RK, Preston AR, Glover GH, Wagner AD. 2011. Associative retrieval processes in the human medial temporal lobe: Hippocampal retrieval success and CA1 mismatch detection. Learn Mem 18:523–528.

Deuker L, Doeller CF, Fell J, Axmacher N. 2014. Human neuroimaging studies on the hippocampal CA3 region -integrating evidence for pattern separation and completion. Front Cell Neurosci 8:1–9.

Dudukovic NM, Preston AR, Archie JJ, Glover GH, Wagner AD. 2011. High-resolution fMRI reveals match enhancement and attentional modulation in the human medial temporal lobe. J Cogn Neurosci 23:670–682.

Duncan KD, Curtis C, Davachi L. 2009. Distinct memory signatures in the hippocampus: intentional states distinguish match and mismatch enhancement signals. J Neurosci 29:131–139.

Duncan KD, Ketz N, Inati SJ, Davachi L. 2012. Evidence for area CA1 as a match/mismatch detector: A high-resolution fMRI study of the human hippocampus. Hippocampus 22:389–398.

Duvernoy HM, Cattin F, Risold P-Y. 2013. The Human Hippocampus. Berlin, Heidelberg: Springer Berlin Heidelberg.

Frankó E, Insausti AM, Artacho-Pérula E, Insausti R, Chavoix C. 2014. Identification of the human medial temporal lobe regions on magnetic resonance images: Human medial temporal lobe landmarks. Hum Brain Mapp 35:248–256.

Hannula DE, Ranganath C. 2008. Medial temporal lobe activity predicts successful relational memory binding. J Neurosci 28: 116–124.

Hunsaker MR, Kesner RP. 2013. The operation of pattern separation and pattern completion processes associated with different attributes or domains of memory. Neurosci Biobehav Rev 37:36–58.

Jenkinson M, Bannister P, Brady M, Smith S. 2002. Improved optimization for the robust and accurate linear registration and motion correction of brain images. NeuroImage 17:825–841.

Jenkinson M, Beckmann CF, Behrens TEJ, Woolrich MW, Smith SM. 2012. FSL. NeuroImage 62:782–790.

Kesner RP. 2013a. An analysis of the dentate gyrus function. Behav Brain Res 254:1–7.

Kesner RP. 2013b. A process analysis of the CA3 subregion of the hippocampus. Front Cell Neurosci 7:1–17.

Kesner RP. 2013c. Role of the hippocampus in mediating interference as measured by pattern separation processes. Behav Proc 93: 148–154.

Kumaran D, Maguire EA. 2006. An unexpected sequence of events: Mismatch detection in the human hippocampus. PLoS Biol 4: e424.

Kumaran D, Maguire EA. 2007a. Match mismatch processes underlie human hippocampal responses to associative novelty. J Neurosci 27:8517–8524.

Kumaran D, Maguire EA. 2007b. Which computational mechanisms operate in the hippocampus during novelty detection? Hippocampus 17:735–748.

Kumaran D, Maguire EA. 2009. Novelty signals: A window into hippocampal information processing. Trends Cogn Sci 13:47–54.

Lacy JW, Yassa MA, Stark SM, Muftuler LT, Stark CEL. 2011. Distinct pattern separation related transfer functions in human CA3/dentate and CA1 revealed using high-resolution fMRI and variable mnemonic similarity. Learn Mem 18:15–18.

Leutgeb JK, Leutgeb S, Treves A, Meyer R, Barnes CA, McNaughton BL, Moser M-B, Moser EI. 2005. Progressive transformation of hippocampal neuronal representations in "morphed" environments. Neuron 48:345–358.

Liang JC, Preston AR. 2015. Medial temporal lobe subregional function in human episodic memory. In: Addis DR, Barense M, Duarte A, editors. The Wiley Handbook on the Cognitive Neuroscience of Memory. Chichester, United Kingdom: John Wiley and Sons, Ltd. pp 108–130.

Lisman JE, Grace AA. 2005. The hippocampal-VTA loop: Controlling the entry of information into long-term memory. Neuron 46:703–713.

Mumford JA. 2007. A guide to calculating percent change with featquery. Retrieved from http://mumford.bol.ucla.edu/perchange_guide.pdf. Last accessed on May 9, 2016.

Rotello CM, Heit E. 2000. Associative recognition: A case of recall-to-reject processing. Memory and Cognition 28:907–922.

Stark CEL, Squire LR. 2001. When zero is not zero: The problem of ambiguous baseline conditions in fMRI. Proc Natl Acad Sci USA 98:12760–12766.

Vinogradova OS. 2001. Hippocampus as comparator: role of the two input and two output systems of the hippocampus in selection and registration of information. Hippocampus 11:578–598.

Yassa MA, Stark CEL. 2011. Pattern separation in the hippocampus. Trends Neurosci 34:515–525.